Available online at www.sciencedirect.com
ScienceDirect
South African Journal of Botany 77 (2011) 755–766
SOUTH AFRICAN JOURNAL OF BOTANY
www.elsevier.com/locate/sajb

Russian wheat aphid biotype RWASA2 causes more vascular disruption than RWASA1 on resistant barley lines

M.A. Jimoh [a], C.E.J. Botha [a,*], O. Edwards [b]

[a] Department of Botany, Rhodes University, P.O. Box 94, Grahamstown 6140, South Africa
[b] CSIRO Ecosystem Sciences, Centre for Environment and Life Sciences, Underwood Avenue, Floreat, WA 6014, Australia

Received 17 March 2011; accepted 30 March 2011

Abstract

We investigated the comparative effects of the feeding damage caused by two Russian wheat aphid (RWA, *Diuraphis noxia* Kurdjumov) biotypes, RWASA1 and RWASA2, on leaves of three RWA-resistant barley (*Hordeum vulgare* L.) lines from the USDA-ARS, and used a South African non-resistant cultivar as control. The relationship between aphid breeding capacity and the structural damage inflicted by the aphids was studied, using wide-field fluorescence and transmission electron microscopy (TEM). Colonies of the two biotypes grew rapidly on all four barley lines during a 10 day feeding exposure but as expected, population size and density were generally lower on the resistant lines than on the non-resistant cultivar. The new South African biotype, RWASA2, bred significantly faster than the original RWASA1 biotype. The feeding and water uptake-related damage sustained by phloem and xylem tissues of the resistant lines suggest that RWASA2 was a more aggressive feeder and caused substantially more cell damage than RWASA1. Examination of wound callose distribution after aphid feeding revealed that high levels of wound callose occurred in non-resistant and in resistant lines. Reduction in aphid population size, as well as ultrastructural damage during feeding by RWA biotypes on resistant lines, signals potential antibiotic and tolerant responses of the barley lines to aphid feeding. We infer from callose distribution and ultrastructural studies, that phloem transport would be substantially reduced in the non-resistant PUMA and to a lesser extent in the resistant STARS lines, which suggests that the STARS lines may be a potential source of RWASA1 and RWASA2-resistance.

Keywords: Antibiosis; Phloem feeding; Resistance-breaking; Tolerance; Xylem and phloem probes

1. Introduction

The Russian wheat aphid (RWA) is a very destructive pest of small grains causing major economic losses to their producers (Walters et al., 1980; Kovalev et al., 1991). Infestation results in loss of effective leaf area, substantial reduction in chlorophyll content and reduced photosynthetic capacity of leaves of host plants, all of which culminate in yield loss (Walters et al., 1980; Fouché et al., 1984; Kruger and Hewitt, 1984). Symptoms of RWA infestation are well documented (see Saheed et al., 2007a; Tolmay et al., 2007).

Previous studies have shown that the effects of feeding by RWASA1 cause severe damage to the phloem as well as to the xylem transport systems within its hosts (Botha and Matsiliza, 2004; de Wet and Botha, 2007; Saheed et al., 2007a, 2007b, 2009, 2010). Several reports have described the pathway of its stylets (see Botha, 2005 and literature cited) to their preferred feeding site, the thin-walled sieve tubes, inflicting severe damage to phloem as well as xylem tissues (Botha and Matsiliza, 2004). Studies by Saheed et al. (2007a, 2007b) in particular, highlighted the structural damage caused by RWASA1 to the vascular tissues of its wheat and barley hosts. These authors showed that RWA, in addition to feeding preferentially on thin-walled sieve tubes, also probes the xylem for water in non-resistant plants and symptomatic leaf streaking, leaf rolling and chlorosis result. Feeding damage by RWASA1

* Corresponding author.
E-mail address: T.Botha@ru.ac.za (C.E.J. Botha).

0254-6299/$ - see front matter © 2011 SAAB. Published by Elsevier B.V. All rights reserved.
doi:10.1016/j.sajb.2011.03.012

was reduced in resistant Betta-*Dn* wheat cultivar compared to its susceptible Betta counterpart (Saheed et al., 2007b).

A second RWA biotype appeared several years ago in South Africa (Tolmay et al., 2007) which is now understood to be resistance-breaking and virulent on existing RWA-resistant wheat lines. A population study (Walton and Botha, 2008) indicated that RWASA2 not only bred faster but also caused more damage to wheat lines than did RWASA1. RWASA2 is apparently unaffected by the *Dn1* resistance gene and may therefore pose a serious threat to small grain production in South Africa.

We recently reported that RWASA2 also breeds faster on resistant and non-resistant barley lines and that the extent of leaf rolling, an important symptom of RWA feeding, correlated with the relative population levels of RWASA1 and RWASA2 on all four barley lines tested (Jimoh et al., 2011). The leaf roll symptom and its development have been suggested to be the result of RWA probing xylem for water (Saheed et al., 2007a, 2007b). Leaf chlorosis, a second symptom of RWA feeding, did not correlate with aphid population levels. Chlorosis symptoms appeared earlier, but were more severe on plants fed upon by RWASA1, the more slowly reproducing of the two biotypes (Jimoh et al., 2011). We surmised that the increased level of chlorosis caused by RWASA1 might be due to differences in either behavioural responses or components of the saliva between the two RWA biotypes.

In the current study, we examine further the relationship between the reproductive rates of the two RWA biotypes, RWASA1 and RWASA2, and the damage they cause to resistant and non-resistant barley lines. Here, we examine feeding-related cell damage after a 10 day feeding exposure period, using wide-field fluorescence and detailed transmission electron microscopy (TEM) to compare and contrast the differences in cellular damage caused by the two RWA biotypes on three selected resistant barley lines. We compare these results to those of our previous study and discuss possible relationships between vascular feeding damage and visible symptoms.

2. Materials and methods

2.1. Aphid colonies

The South African biotypes of the Russian wheat aphid, RWASA1 and RWASA2, were obtained from the Agricultural Research Council (ARC), Small Grain Institute, Bethlehem, South Africa. Their colonies were maintained on young susceptible barley (*Hordeum vulgare* L.) cv. Clipper (Saheed et al., 2007a) in separate controlled environment cabinets (Conviron S10H, Controlled Environment Ltd., Winnipeg, Manitoba, Canada). The colonies were maintained at a day time maximum of 24 °C and 66% relative humidity (RH) and at 22 °C, 60% RH (night), with a 14-h photoperiod. The light source was a combination of fluorescent tubes (F48T12.CW/VHO 1500, Sylvania, Danvers, MA) and frosted incandescent 60 W bulbs (Phillips, Eindhoven, The Netherlands), with a PAR level of 250 $\mu mol^{-2}\ s^{-1}$ 30 cm below the light source. Fresh pots of two-week old feeder plants were introduced into the breeding cages of each biotype, at intervals of two weeks. Each pot was usually infested with 30 apterous RWAs on an older leaf segment which was placed at the axils of the feeder plants, thereby allowing aphids' free movement and settlement. In order to prevent release of the aphids into the environment, discarded treatments were placed in black polythene bags and sprayed with aerosol pyrethroid insecticide (SC Johnson and Sons (Pty) Ltd., South Africa).

2.2. Barley lines

Four barley lines were used in this study. These were STARS-0502B (PI 47541), STARS-9301B (PI 573080) and STARS-9577B (PI 591617), which were developed by the United States Department of Agriculture, Agricultural Research Service (USDA-ARS), Stillwater, Oklahoma. These are known to be resistant to several US RWA biotypes (Webster et al., 1993; Mornhinweg et al., 1995, 1999, 2006; Puterka et al., 2006). PUMA, a widely cultivated barley cultivar in South Africa was used as a non-resistant line. Seeds of the four lines were obtained from the ARC, Bethlehem, South Africa.

Seeds were pre-germinated in Petri dishes and sown, one seedling per pot, in potting soil (2:1:1; garden soil:compost: vermiculite mixture) in 17 cm-diameter plastic pots in a greenhouse maintained at 20–30 °C for 1 week. The seedlings were sprayed with aerosol pyrethroid insecticide to kill any insects that may have colonised them while in the greenhouse and were exposed to fresh air for another 24 h (Jyoti et al., 2006), then moved to the growth cabinets (Conviron) where they were grown for 2 weeks, to reach 2–3 leaf stage before being manually infested with the aphids. Half strength Long Ashton nutrient solution (Hewitt, 1966) was applied 3 times per week.

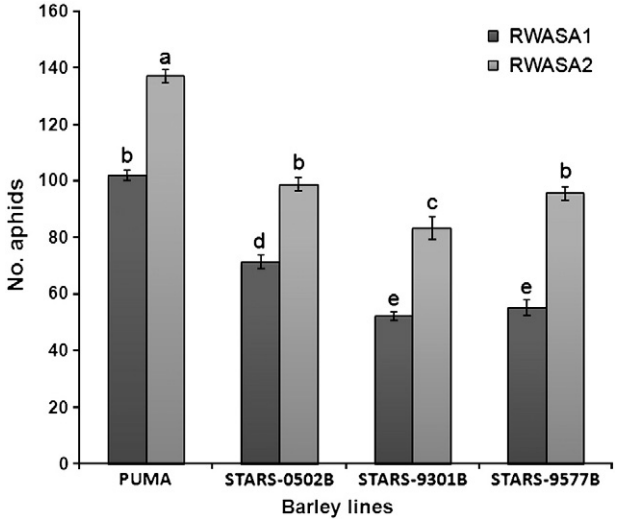

Fig. 1. Population growth data for RWASA1 and RWASA2 on four barley cultivars over a 10-day infestation period, all treatments starting with 10 aphids. As expected, RWASA2 reproduced faster than RWASA1 on non-resistant as well as on the resistant lines. Highest aphid numbers were recorded on non-resistant PUMA for both RWASA1 and RWASA2, but were reduced on STARS-9301B. Bars with different letters indicate significantly different homologous groups at the 0.05 level using Tukey *post hoc* test of a 2-way ANOVA (n = 10).

Table 1
Population density (cm^{-2} of leaf area) of RWASA1 and RWASA2 feeding on barley leaves (±standard error of mean).

	Aphid biotype	
Barley line	RWASA1	RWASA2
PUMA	48.67±0.90	65.33±1.12
STARS-0502B	34.05±1.15	47.14±1.12
STARS-9301B	24.95±0.74	39.81±1.91
STARS-9577B	26.38±1.37	45.62±1.09

2.3. Experimental design

The barley lines were tested against the two aphid biotypes (RWASA1 and RWASA2) using clip cages (Saheed et al., 2009), which were used to enclose a 3 cm-long segment of either the second or the third leaf above the coleoptile of each experimental plant. A leaf segment from feeder plants containing 10 apterous aphids was carefully introduced into the clip cage for each biotype. Ten replicates of each treatment combination (2 aphid types × 4 plant types) were set up, making a total of 80 plants. Experimental procedures were repeated twice. The aphids were allowed 24 h to transfer and settle on the confined leaf. At ten days after infestation (DAI), the clip cages were carefully removed and the aphid population counted, using a hand lens. Leaf segments from regions where the aphids had been feeding were thereafter processed for either fluorescence or transmission electron microscopy (TEM) studies. Control (uninfested) leaf materials were collected at the same time.

2.4. Preparation of leaf material for wide-field fluorescence studies

After clip cage removal, the confined portion on each leaf was marked with a soft tip marker. Feeder leaves were severed and immediately transferred into Ca^{2+}-free buffer (10 mM 2-[morpholino] ethanesulfonic acid, MES), 0.5 mM $MgCl_2$, 0.5 mM KCl and 125 mM mannitol, adjusted to pH 7.2. The abaxial surface of the marked feeding area was gently scraped under the MES buffer on a glass plate using a sharp, single-edge carbon steel razor blade (Agar Scientific, USA), in order to remove the cuticle and the underlying epidermal tissue, thereby exposing "windows" into the mesophyll and underlying vascular tissues. The scraped leaves were mounted on slides in Ca^{2+}-free MES buffer and stained by applying a few drops of the aniline blue fluorochrome (4′4-[carbonyl bis (benzene 4,1-diyl) bis (imino)] bis benzensulphonic acid) (Biosupplies Australia Pty Ltd). The sections were covered with cover slips and incubated in the dark for 30 min at 20 °C. Thereafter, the leaf segments were washed in fresh Ca^{2+}-free MES buffer and examined for callose fluorescence under UV light using an

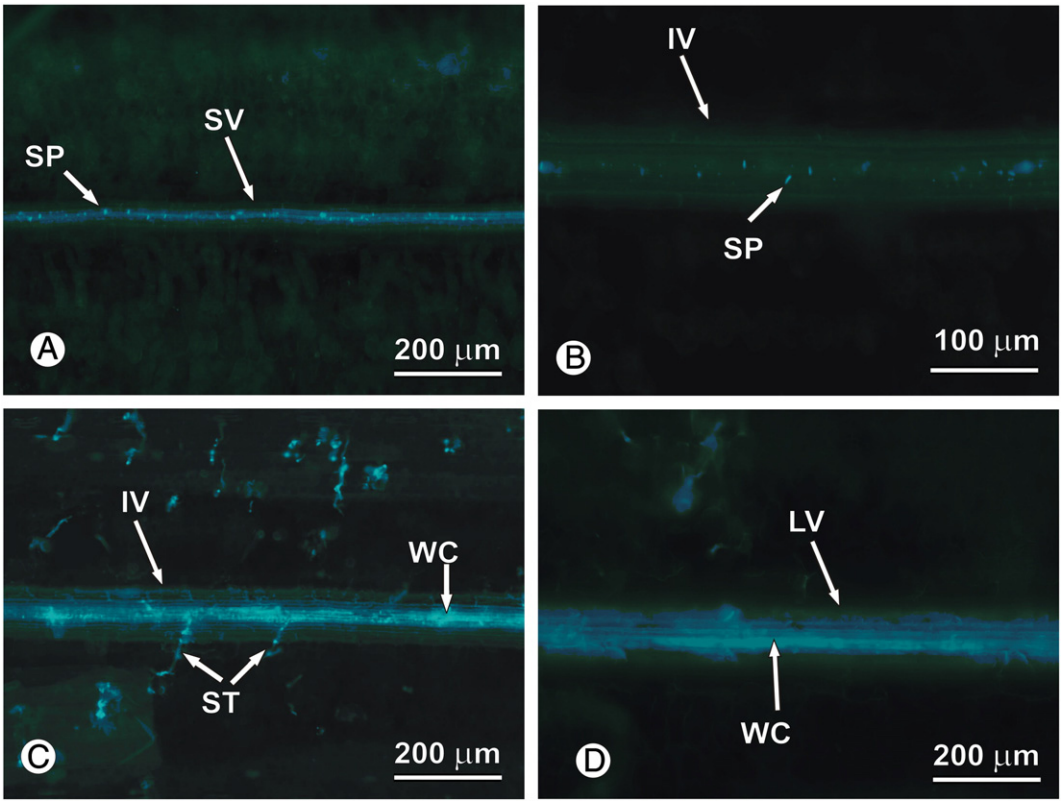

Fig. 2. Wide-field fluorescence micrographs, showing distribution of wound callose in control (A–B) and non-resistant PUMA (C–D) after a 10 day feeding period. A and B. Longitudinal sections of aniline blue stained uninfestedcontrol leaves, showing the distribution of callose. A.Small vein (SV) from the leaf of the non-resistant PUMA line. B. Part of an intermediate vein (IV) from STARS-9301B leaf. Callose formation is minimal and restricted to the sieve plate regions along the lengths of the veins. C–D. Wound callose distribution after a 10 day feeding exposure on the non-resistant PUMA leaves. Sustained feeding by RWASA1 (C) and RWASA2 (D) induced extensive damage.

Olympus BX61 wide-field fluorescence Digital Imaging Microscope (Olympus, Tokyo, Japan supplied by Wirsam Scientific, Johannesburg, South Africa), using a narrow-band aniline blue specific filter cube (excitation: 425–440 nm; emission of 475 nm). The aniline blue fluorochrome dye is specific for callose. High-resolution images were collected, saved in a database using analySIS (Soft Imaging System GmHb, Germany). Selected images were imported as 600 pixels per inch 32 bit CMYK bitmaps to CorelDRAW.

2.5. Treatment of the leaf material for TEM

Leaf segments from the control and infested plants were cut into strips in cold fixative made up of 6% paraformaldehyde–glutaraldehyde (v/v) in 0.05 M sodium caccodylate buffer using a sharp, clean and single-edge razor blade. The strips were trimmed and diced into smaller pieces (approximately 2 × 3 mm in size) and placed in small vials and subjected to a very slight vacuum (17,000 kg/m s^2) for 1 h after which the fixative was changed and

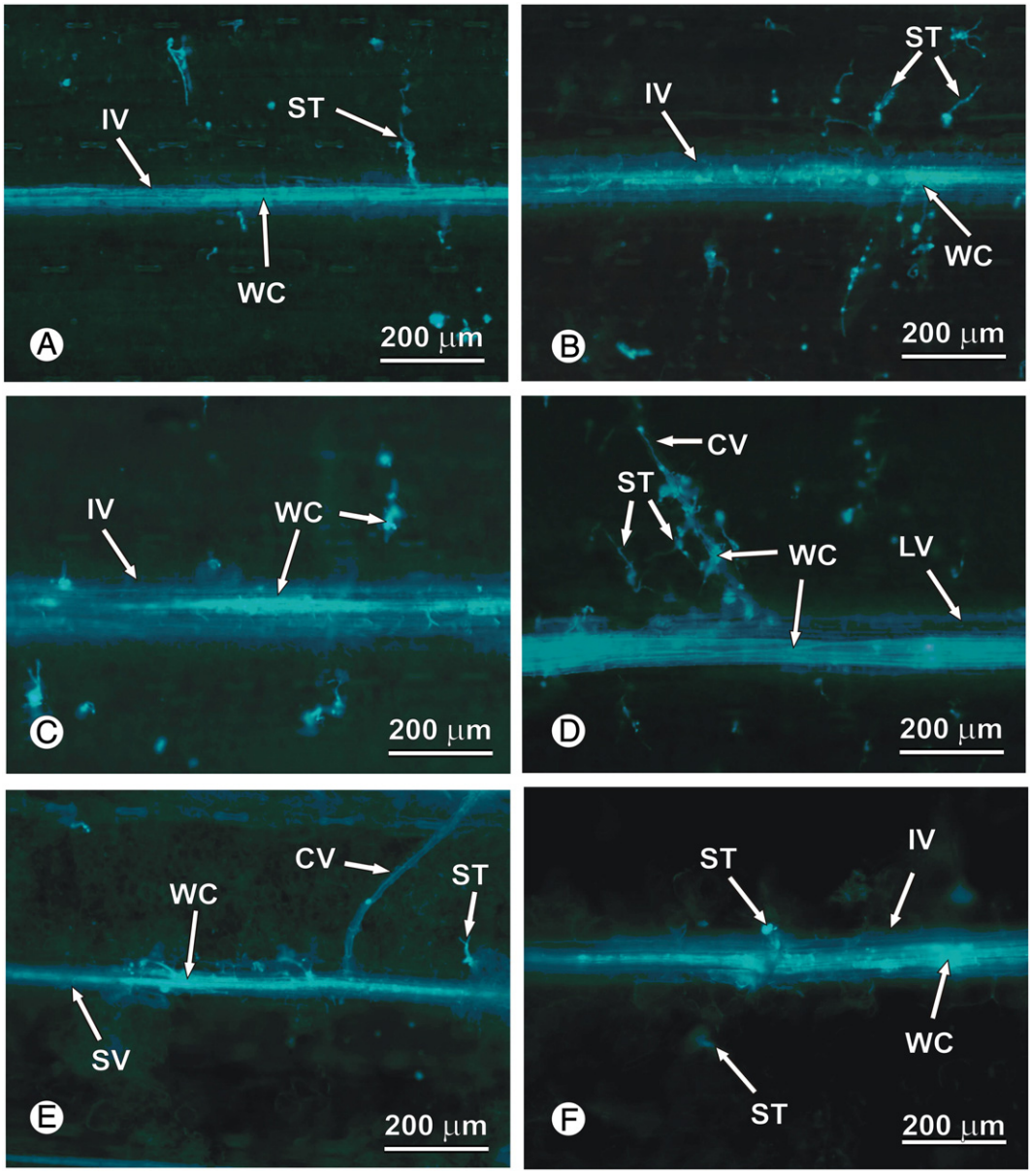

Fig. 3. Wide-field fluorescence micrographs, showing distribution of wound callose in resistant STARS lines after a 10 day feeding period. A–F shows the distribution of wound callose in the leaves of the resistant STARS lines, on which RWASA1 (LHS of plate) and RWASA2 (RHS of plate) were feeding for 10 days. A. STARS-0502B. Part of an intermediate vein (IV) from leaf fed on by RWASA1. The stylet track (ST) is associated with an extensive wound callose deposit in the vein. B. STARS-0502B. An intermediate vein exposed to RWASA2 feeding. The callose-positive stylet tracks were associated with an aphid colony that probed the mesophyll extensively, thereby inducing the formation of widespread wound callose within this vein (compare callose distribution in Fig. 3A and B). C. STARS-9301B. Intermediate vein, probed by RWASA1. D. Part of a large vein (LV) and a connecting cross vein (CV) from STARS-9301B fed on by RWASA2. Extensive, intense staining suggests more aggressive feeding by RWASA2 than was the case with RWASA1 on this cultivar. E. STARS-9577B. A small vein probed by RWASA1. Intense callose fluorescence (WC) is evident in this vein, but RWASA2 feeding on this cultivar (Fig. 3F) revealed more widespread callose formation on the same cultivar. Note all visible sieve tubes and associated vascular parenchyma cells have been obliterated.

the vials were transferred to a refrigerator maintained at 4 °C and left overnight. The leaf tissues were washed in three changes of cold 0.05 M sodium caccodylate buffer and transferred to cold 2% osmium tetroxide in 0.05 sodium caccodylate buffer in the refrigerator overnight, washed in cold buffer and dehydrated in a cold graded ethanol series, followed by two changes in 100% propylene oxide. Spurr's (1969) epoxy resin was used in embedding the leaf tissues. Ultrathin sections (silver to gold) were cut using a diamond knife (Drukker, The Netherlands). The sections were collected on 300 mesh copper grids (SPI Suppliers, Philadelphia, USA) and stained with 2% uranyl acetate in distilled water followed by Reynolds's lead citrate. They were viewed and imaged at 80 kV, using a JEOL JEM 1210 transmission electron microscope (JEOL, Tokyo, Japan). The images taken were thereafter imported into CorelDRAW software (version 12) for presentation.

2.6. Aphid population data analysis

A 2-way factorial ANOVA was used to examine the differences in the population growth of the two aphid clones on the four barley lines using Statistica version 8.1 (StatSoft, 2007). Aphid types and barley lines were the independent variables while the number of aphids constituted the dependent variable. Prior to analysis, homogeneity of variances and normality of the aphid's population growth data were examined using Levene's and Shapiro–Wilk's tests respectively (Johnson and Wichern, 2002). Homogenous groups were identified using Tukey *post hoc* test at 5% level of significance (StatSoft, 2007). Population density per cm^2 of leaf area was calculated by dividing the number of aphids enumerated for each replicate with the average area of the leaf segment within the clip cage (2.1 cm^2), on which aphids were confined.

3. Results

3.1. Infestation symptoms

Feeding by RWASA1 and RWASA2 resulted in visible damage to the leaves of non-resistant PUMA, which was less evident in the three resistant lines (STARS-0502B, STARS-9301B and STARS-9577B). Symptoms such as chlorosis, necrosis, longitudinal yellow streak and leaf rolling were observed on PUMA at 5 DAI, while the resistant lines only showed few chlorotic and necrotic spots within the 10-day experimental period (data not included). These results are consistent with symptoms observed at this stage of infestation in previous experiments (Jimoh et al., 2011).

3.2. General observations on aphid population growth

Populations of the two biotypes (RWASA1 and RWASA2) increased substantially from the 10 apterous aphids at the beginning of the experiments on both non-resistant and resistant lines (Fig. 1, Table 1) until 10 DAI, when experiments were terminated for collection of leaf material for the fluorescence microscopy and TEM studies of vascular damage. There were significant differences in the mean number of aphids between the two aphid biotypes ($F_{1,72}=343.4$, $p=0.0001$) and among the four barley lines ($F_{3,72}=159.2$, $p=0.0001$). However, we found

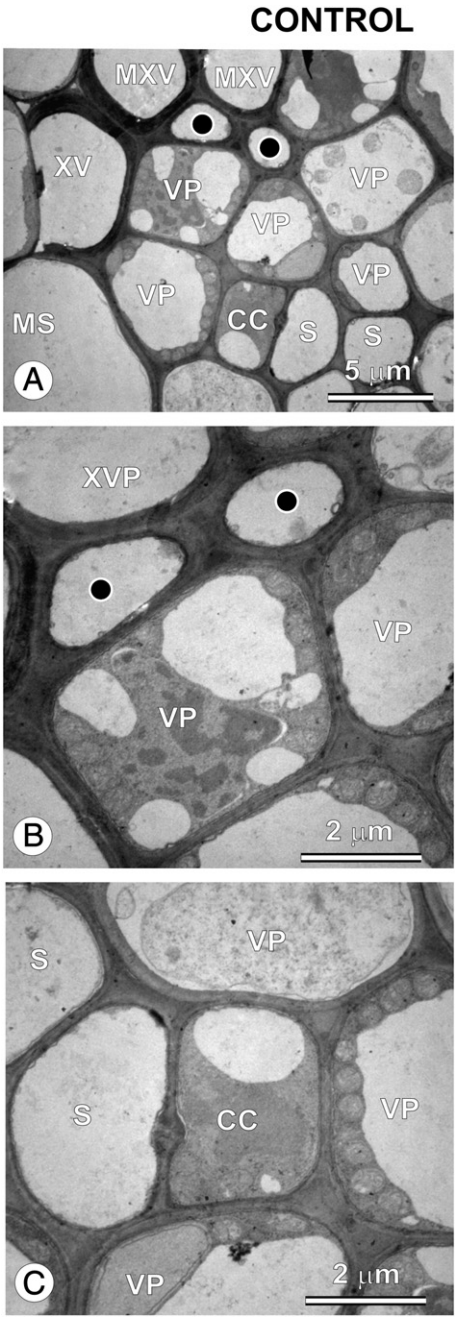

Fig. 4. TEM micrographs illustrate fine structure details from an intermediate vascular bundle in control leaves. A. Part of the phloem, showing two thick-walled sieve tubes (solid dots) next to the metaxylem vessels (MXV). Several thin-walled sieve tubes (S), an associated companion cell (CC) and vascular parenchyma (VP) are also visible. B. Detail showing two thick-walled sieve tubes and associated vascular parenchyma. C. Thin-walled sieve tubes to the left and a companion cell with lateral sieve area interconnecting to a sieve tube. Note that there is no visible evidence of plasmolysis or cell disruption in these control images. Abbreviations. BS = bundle sheath cell; CC = companion cell; MS = mestome sheath cell; MXV = large metaxylem vessel; S = thin-walled sieve tube; SM = salivary material; SS = stylet sheath; VP = vascular parenchyma cell; XV = xylem vessel; solid dot = thick-walled sieve tube.

no significant difference in the interaction between the aphids and cultivars ($F_{3,72}=2.3$, $p=0.082$). This was consistent with previous experiments, indicating that RWASA2 consistently outperformed RWASA1 on all lines and that resistance in barley suppressed population growth of both aphid biotypes. As expected, the non-resistant PUMA line supported the largest population for both biotypes after the 10-day experimental period. In contrast, RWA feeding on STARS-9301B resulted in

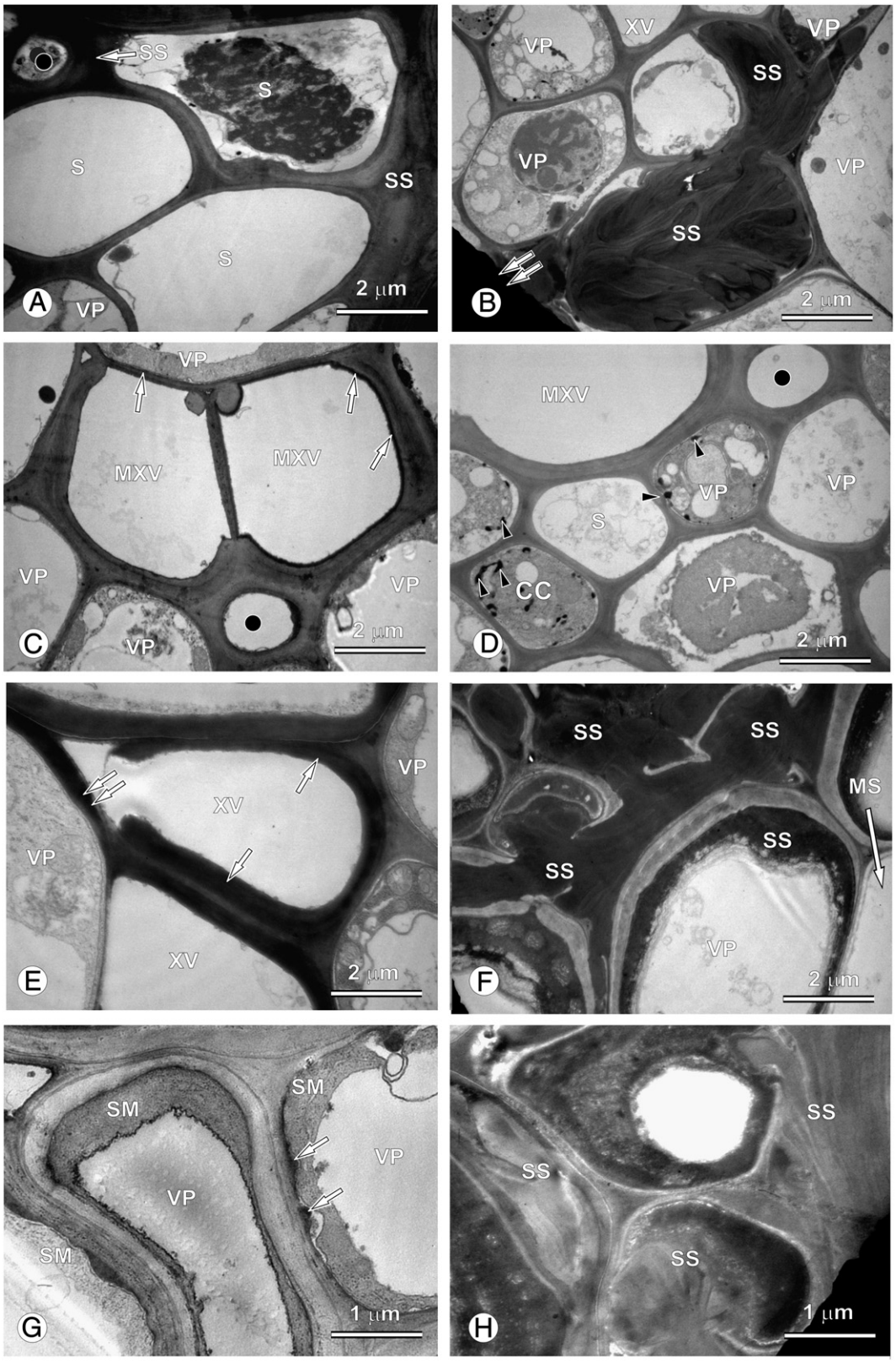

the lowest population (Fig. 1) for both RWASA1 and RWASA2 (about 50 and 85 aphids respectively). PUMA (infested with RWASA1), STARS-0502B (infested with RWASA2) and STARS-9577B (infested with RWASA2) were not significantly different at 5% confidence level. Similarly, there was a lack of significance for both STARS-9301B and STARS-9577B infested with RWASA1. The trend of the population growth of the two biotypes among the resistant lines was thus STARS-0502B > STARS-9577B > STARS-9301B.

3.3. Callose distribution

The fluorescence micrographs (Figs. 2 and 3) provide an overview of the damage caused due to aphid infestation as shown by the distribution of callose within control (uninfested) and infested leaves. In the longitudinal veins of uninfested non-resistant PUMA plants (Fig. 2A), callose deposition was limited and was usually associated with sieve plates, lateral sieve areas, pore plasmodesmal units between sieve elements and their associated parenchymatous elements, including companion cells. A similar observation, like in uninfested PUMA, was found in uninfested resistant STARS-9301B (Fig. 2B). However, during exposure of non-resistant PUMA to RWASA1 (Fig. 2C) or RWASA2 (Fig. 2D), callose deposition and distribution were generally similar and extensive in sieve tubes as well as the sieve tube lumina.

Callose distribution in small and intermediate veins of the resistant STARS lines is illustrated in Fig. 3A–F. Where RWASA1 (Fig. 3A, C, and E) and RWASA2 (Fig. 3B, D and F) were feeding, there appears to be substantial levels of callose deposition within the veins and positive callose reactions were associated with the stylet tracks as well (see ST, Fig. 3A–F) in all the sections examined. What is interesting is the similarity of salivary deposition reactions caused by RWASA1 and RWASA2, as neither leaves with high aphid population (typified by STARS 0502B, Fig. 3A and B respectively) nor leaves on which smaller aphid populations existed (typified by STARS 9301B, Fig. 3C and D respectively) showed contrasting callose distribution at the end of the 10-day experimental period. It was however evident that the sieve tubes in small, intermediate and large veins contained massive callose deposits, which is an indication of severe damage. When aphids probed near to, or in cross veins, all sieve tubes, sieve plates and pore plasmodesmal units contained callose.

3.4. Ultrastructural damage

3.4.1. Control tissue

Fig. 4A–C shows details of the vascular tissue in a large intermediate vascular bundle from control (uninfested) leaves. Here, two thick-walled (solid black dots) and several thin-walled sieve tubes (S) are visible (Fig. 4A). All cells appear normal in these sections. Characteristically, thin-walled sieve tube-companion cell complex (S and CC respectively) forms the bulk of the phloem tissues in the vascular bundles (Fig. 4B–C). These images are typical of those obtained from the control tissues in non-resistant as well as resistant lines.

3.4.2. RWASA1 and RWASA2-related feeding damage on non-resistant line

Feeding-related damage attributable to RWASA1 feeding and probing of vascular tissues of leaves of the non-resistant PUMA is shown in Fig. 5A–D. The aphids primarily probed and fed in the sieve tubes of the phloem. As in earlier studies, we noted that RWA feeds more extensively from the thin-walled than from the thick-walled sieve tubes. RWASA1 feeding resulted in severe damage to the phloem and copious evidence of salivary material (SM) deposition in thin-walled sieve tubes (Fig. 5A) occurred which in most cases, resulted in disruption of the sieve tube cytoplasmic matrix. Stylet sheath material (SS) completely obliterated a vascular parenchyma (VP) cell and saliva was present in a thin-walled sieve tube as well (Fig. 5B).

Probing of the xylem, irrespective of the aphid and barley cultivar, always had similar effects — watery ejecta preceded presumed water ingestion and the resultant watery saliva rapidly coated the inner face of vessels as well as half-bordered pits between the xylem and the associated parenchyma (Figs. 5C, E, and 6A, B, D and E). The electron-dense material can be easily identified in Fig. 5C due to RWASA1 feeding and in Fig. 5E due to RWASA2. Little, if any, discernible difference exists in salivary material deposition, unlike the

Fig. 5. TEM images illustrate the typical damage caused by RWASA1 (A–D) and RWASA2 (E–H) feeding on non-resistant PUMA leaves. A. The salivary sheath (SS, left and right) shows the intercellular passage of stylets, next to a saliva-containing (punctured) thick-walled sieve tube (left, solid dot) and thin-walled sieve tube (right). Granular salivary deposit (SM) is present in the adjacent sieve tube. The two thin-walled sieve tubes (S) below are undamaged. B. Massive saliva deposits (SS) resulted from an extensive inter- and intracellular probe within the vascular tissues in this bundle, which disappears (double arrow at lower left) under the TEM grid bar. A vascular parenchyma cell and an adjacent thin-walled sieve tube were disrupted due to the aphid's probing. C. Part of a small intermediate vascular bundle. Here, the metaxylem is lined by electron-dense saliva (arrows), presumably deposited after saliva ejection, prior to the aphid drinking xylem sap. Note the electron-dense pit membrane between the metaxylem vessels — impregnated by watery saliva, ejected during the probe of these xylem vessels. D. Thin-walled sieve tubes, associated parenchyma cells, including companion cells. Here, damage and disruption of the cytoplasm (electron-dense regions in cytoplasm (arrowheads)) have resulted from feeding. E. A xylem vessel in an intermediate vein contains salivary ejecta, deposited prior to uptake of xylem sap and water by the aphid. The watery saliva has impregnated the cell walls. Note the pit membrane between the vessels which has been occluded (double arrows). F. Extensive and massive damage to the vascular tissue in a large vein. All the cells are obliterated and contain copious salivary deposits, rendering the vascular tissue non-functional. G. Here, granular, partly electron-lucent salivary deposits (SM) line the wall of the parenchyma cell. Saliva was deposited on and in the cell walls. Electron-dense saliva deposits are associated with the plasma and vacuolar membranes within this vascular parenchyma cell. H. Here, copious salivary ejection has resulted in cell obliteration. Abbreviations. BS = bundle sheath cell; CC = companion cell; MS = mestome sheath cell; MXV = large metaxylem vessel; S = thin-walled sieve tube; SM = salivary material; SS = stylet sheath; VP = vascular parenchyma cell; XV = xylem vessel; solid dot = thick-walled sieve tube.

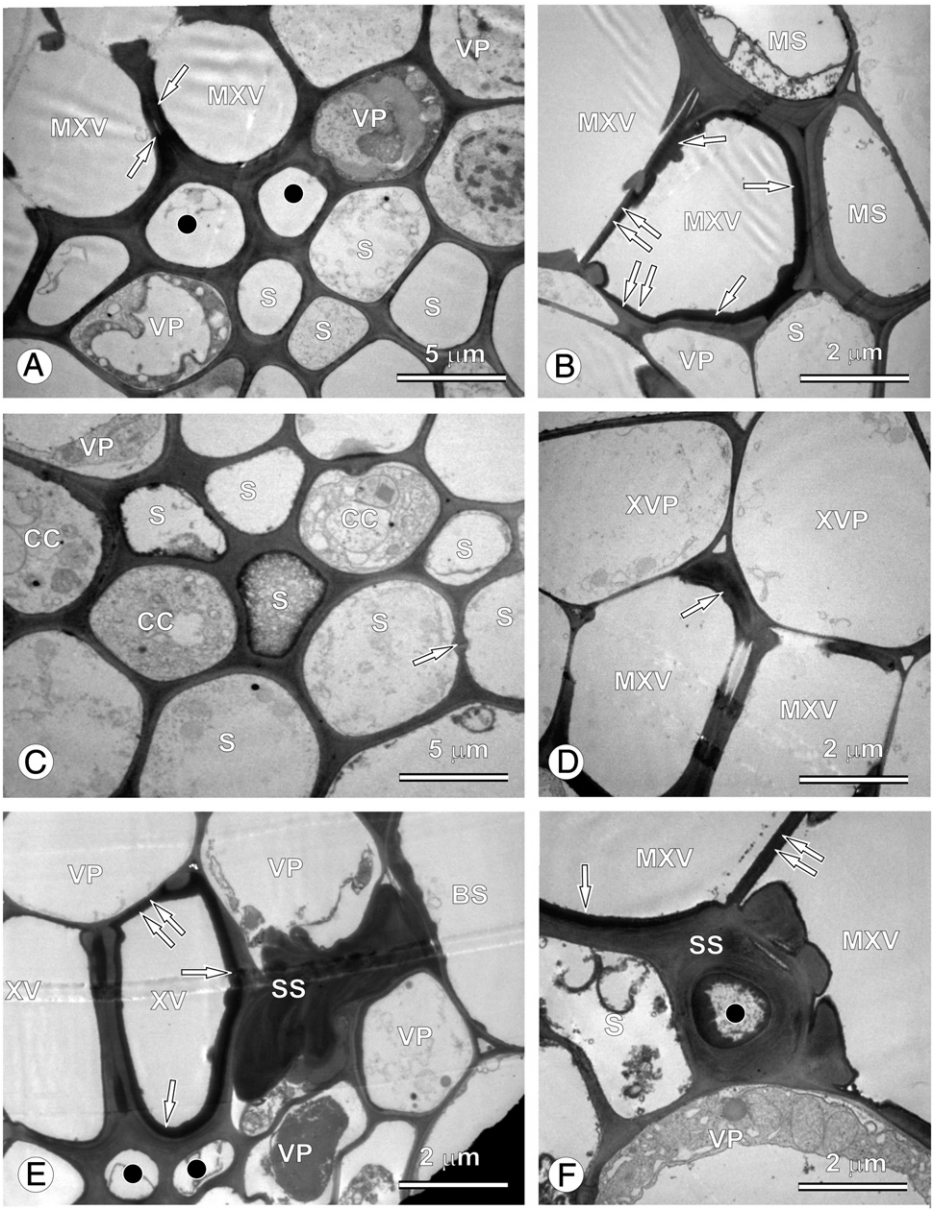

Fig. 6. Damage caused by RWASA1 feeding on resistant STARS lines. A. STARS-0502B. Detail of part of a large vein. Several thick-walled sieve tubes (solid dots) appear undamaged. Vascular parenchyma (VP, lower left) cell is plasmolysed, as a result of stylet puncture. The probed metaxylem contains electron-dense saliva lining the cell walls (arrows). Note that pit membranes between the pair of metaxylem vessels (top centre) are unoccluded. B. STARS-0502B. Electron-dense saliva lines the walls of metaxylem vessels (arrows). Pit membranes (double arrows) are occluded by saliva. Plasmolysed mestome sheath cell (upper right) was possibly punctured during this xylem probe. Surrounding xylem parenchyma cells appear unaffected. C. STARS-9301B. Detail of phloem of a large or intermediate bundle with evidence of RWASA1 feeding. Two central thin-walled sieve tubes contain electron dense saliva and the surrounding vascular parenchyma cells are plasmolysed. D. STARS-9301B. Metaxylem vessels in an intermediate vascular bundle. Here, salivary deposits line the inner face of the cell walls and pit membranes are occluded by electron-dense saliva. E. STARS-9577B. Salivary sheath (SS) from inter- and intracellular probes, terminating in the xylem. Several cells were obliterated during this probe. Thick wall sieve tubes and associated vascular parenchyma cells are plasmolysed. Xylem vessel cell walls (arrows) and pit membranes are occluded (double arrows). F. STARS-9577B. Part of a saliva-lined and obliterated thick-walled sieve tube, adjacent to a pair of metaxylem vessels (above). Metaxylem and pit membranes (double arrows) are lined with saliva. Abbreviations. BS = bundle sheath cell; CC = companion cell; MS = mestome sheath cell; MXV = large metaxylem vessel; S = thin-walled sieve tube; SM = salivary material; SS = stylet sheath; VP = vascular parenchyma cell; XV = xylem vessel; solid dot = thick-walled sieve tube.

reported difference between BCA and RWASA1 (Saheed et al., 2007a). Thick-walled sieve tube lumen (Fig. 5C) contains saliva, suggesting that the aphid in question also probed the cell as well. Thin-walled sieve tubes are often plasmolysed (Fig. 5D) and contain granular material. Companion cells (CC) and phloem parenchyma (VP) contain saliva (dark matrix) and are plasmolysed.

Fig. 5E–H illustrates aspects of feeding and resultant cell damage in vascular tissues probed by RWASA2. Cells were generally more extensively probed by RWASA2 than under

RWASA1 feeding. Fig. 5E–F shows salivary sheaths that mark the path of an extensive aphid probe. Xylem cell walls (arrows, Fig. 5E) and the half-bordered pit pairs (double arrows) contain electron-dense saliva. In Fig. 5F, salivary sheath material (SS) obliterates all cells in view. Phloem parenchyma (VP) which was probed during penetration by the stylet sheath of RWASA2 is obliterated and ensheathed with salivary material (SM and arrows, Fig. 5G). Inter- and intracellular probes are evident (Fig. 5H).

3.4.3. Feeding damage by RWASA1 and RWASA2 on resistant lines

Fig. 6 shows examples of feeding-related damage caused by RWASA1 in the resistant STARS lines. Here, damage to xylem (Fig. 6A, B, D and E) and phloem elements (Fig. 6C, E and F) as well as deposition of salivary sheaths (SS, Fig. 6E and F) is evident, but not as extensive as observed for both biotypes on the non-resistant PUMA (see Fig. 5). Cells along the probe pathway contain saliva as well as granular material, but cell plasmolysis and disruption are less severe (Fig. 6A and C) compared to RWASA2 feeding damage. Xylem probes reveal amorphous electron-dense salivary deposits lining the lumen of vessels, which effectively seal these vessels from surrounding vascular parenchyma (Fig. 6B and E) and phloem tissues (see Fig. 6E and F). However, xylem vessels of STARS-9301B appear unaffected, the half-bordered pit pairs and their pit membranes are not occluded by salivary deposits (Fig. 6D).

RWASA2 feeding-related damage on the STARS lines was more extensive than under RWASA1 feeding (Fig. 7A–F). Here, xylem damage (Fig. 7A and B) and obliteration of a thick-walled sieve tube (SS, Fig. 7B and D) are visibly more extensive compared to the situation under RWASA1 feeding (see Fig. 6B, D and E). Both thin-walled sieve tubes and parenchyma are obliterated or are ensheathed by saliva (see sieve tubes, S in Fig. 7C and E) — often resulting in dense saliva-related aggregates in sieve tubes and companion cells (CC, Fig. 7E). Cytoplasm shows evidence of extensive more severe plasmolysis (Fig. 7B, C, and D) than under RWASA1 infestation (Fig. 6A and C). Probed thin-walled sieve tubes of STARS-9577B show severe plasmolysis (Fig. 7F) and occlusion of pore plasmodesmatal units (arrows, Fig. 7E) and sieve area pores (arrows, Fig. 7F).

4. Discussion

4.1. Population growth of the aphids on host plants

The population growth measurements for RWASA1 and RWASA2 obtained in this study were consistent with those obtained from a 15-day time-course study on the same four barley lines (Jimoh et al., 2011), and with other studies focused only on RWASA1 (Saheed et al., 2007a). RWASA2 consistently outperformed RWASA1 on both resistant and non-resistant lines, very similar to their relative performance on resistant and susceptible wheat (Walton and Botha, 2008). None of the virulent RWA biotypes studied overseas shows a difference in performance on barley in addition to wheat (Puterka et al., 2007; Edwards, unpublished data), suggesting that the virulence mechanism in RWASA2 is unique to South Africa. The performance of both aphid biotypes was reduced on all three resistant lines, but the population levels of RWASA2 on the resistant lines were similar to that of RWASA1 on the susceptible line PUMA.

4.2. Both biotypes caused extensive cellular damage on the non-resistant line PUMA

Vascular cell damage was so extensive after 10 days of RWASA1 or RWASA2 feeding on the non-resistant line PUMA that it was impossible to determine whether there were any differential effects from the two biotypes. Upon reaching the vascular bundle, aphid stylets often penetrate the vascular parenchyma prior to penetration of xylem elements and phloem tissues (Evert et al., 1973; Matsiliza and Botha, 2002; Botha and Matsiliza, 2004; Botha, 2005; Saheed et al., 2007a, 2007b). Xylem is targeted for water (Tjalingii, 1994). RWA saliva has been previously observed in both xylem and phloem elements (Saheed et al., 2007b). On the non-resistant PUMA, aggressive inter- and intracellular probing by the two biotypes resulted in severe cell disruption and or frequent cell obliteration of all three tissue types. In the xylem, saliva must impair water and solute exchange by blocking the half-bordered pit pairs (Saheed et al., 2007b), which may contribute to the leaf rolling symptoms caused by RWA feeding. In the phloem, salivary ejecta may cover lateral sieve area pores between adjacent sieve tube members as well as initiating or causing deposition of wound callose. On PUMA, large swaths of phloem tissue contained aphid-induced callose within the sieve plates, lateral sieve areas and pore plasmodesmal units. The resulting reduction in phloem transport capacity could exacerbate leaf chlorosis, local necrosis and the longitudinal streaks commonly associated with prolonged RWA feeding (Saheed et al., 2007b).

4.3. Cellular damage was greatly reduced on the resistant lines

The vascular cell damage caused by each biotype was substantially reduced on all the resistant lines compared to what was observed on the non-resistant line PUMA. With overall damage levels reduced, it was possible to compare the damage caused by the two biotypes and it was clear that RWASA2 caused more cellular damage than RWASA1. On all three resistant lines, some vascular parenchyma cell disruption was evident but the majority of these cells appeared relatively unaffected. However, plasmolysis was often evident suggesting that functional disruption had taken place. Xylem damage was also reduced on all three resistant lines, but was particularly reduced on STARS-9301B (see Figs. 6C and 7D). Phloem cell damage on the resistant lines was more extensive under RWASA2 feeding than with RWASA1 infestation.

The reduction in cellular damage on resistant lines was not reflected in the extent of callose deposition observed on these lines. No obvious differences in callose distribution were detectable between the resistant and susceptible lines, nor as a

consequence of feeding between the RWASA1 and RWASA2 biotypes. In contrast, wheat cultivars containing the *Dn1* resistance gene exhibit substantial reductions in callose deposition due to RWA feeding, and RWASA2 induces more callose than RWASA1 (de Wet and Botha, 2007; Saheed et al., 2007b; Walton and Botha, 2008). Hence, reduced callose deposition can be, but is not by necessity an indicator of resistance to RWA.

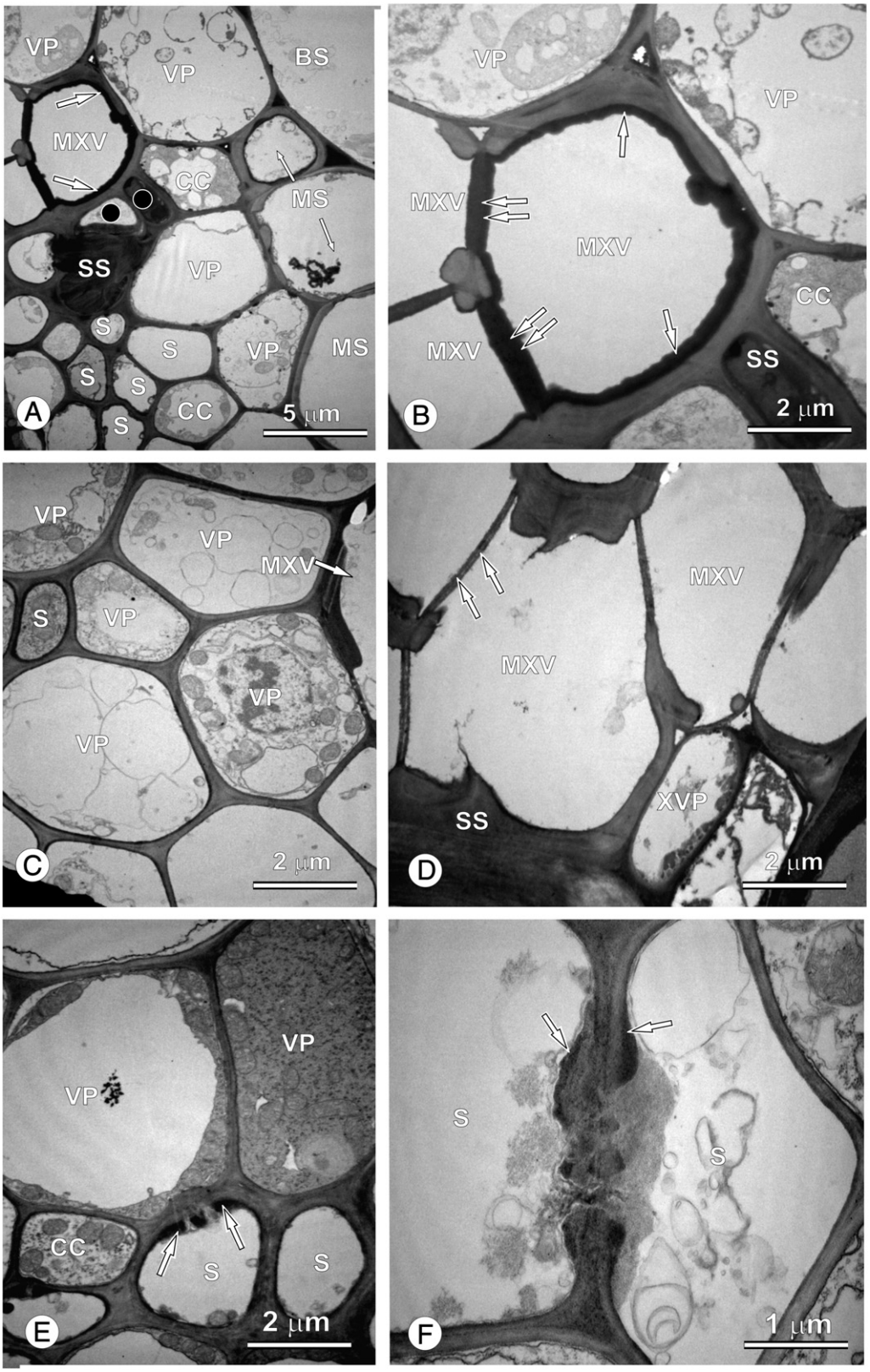

4.4. The relationship between population growth and feeding damage

In this study, aphid population growth was significantly influenced by both factors tested: resistance and aphid biotype. Cellular damage resulting from aphid feeding was also affected by both factors, but to a different degree. RWASA2 population levels were higher than those of RWASA1 on all plants tested, and the presence of resistance suppressed RWASA2 populations to a level resembling those of RWASA1 on the susceptible PUMA plants. In contrast, cellular damage by RWASA2 on the three resistant lines was far lower than that caused by RWASA1 on PUMA plants. Hence, the results of this study do support the conclusion from previous work (Jimoh et al., 2011) that resistance in these three barley lines has an antibiosis effect on the two RWA biotypes, but they also suggest that the resistant lines are more tolerant of RWA feeding. That is, the level of suppression of cellular damage on the resistant lines exceeds what one would expect from the antibiotic effects on aphid population growth. The results of a previous study (Jimoh et al., 2011) showed that the amount of leaf roll, a visible symptom of RWA feeding in barley, could be explained simply by aphid population levels, irrespective of biotype. However, the amount of leaf roll caused by RWASA2 on resistant lines in this previous study was approaching the maximum leaf roll score of '3', so higher measurements for RWASA1 on the susceptible line PUMA were not possible. Therefore, our conclusion that there are both antibiosis and tolerance effects of the resistance in these barley lines is consistent with the results of both studies. Tolerance has also been put forward as a major component of resistance in these same STARS lines in tests against RWA biotypes in the USA (Mornhinweg et al., 2006; Puterka et al., 2006).

By comparing information on visible symptoms (Jimoh et al., 2011) to the levels of cellular damage observed herein, we can reasonably conclude that the leaf rolling symptom arises as a consequence of cell damage to vascular tissue. Apoplasmic and symplasmic isolation of xylem and phloem vessels by salivary secretions could result in leaf roll, which is also a symptom of water stress (Saheed et al., 2007b). The threshold of cellular damage necessary to induce maximum leaf roll appears to be quite low, suggesting that leaf roll may not by itself be a suitable measure of plant susceptibility to RWA. Leaf roll and chlorosis are often used together to assess RWA resistance in breeding programmes, but chlorosis has also been found to be poorly correlated with resistance (Puterka et al., 2006; Jimoh et al., 2011). As such, assessments of resistance should probably include measurements of plant biomass.

Unfortunately, this study has not provided additional insights as to the biological differences between RWASA1 and RWASA2. RWASA2 did cause more cellular damage on each resistant plant, but this can be explained by this biotype's correspondingly higher growth rates. It could be that the increased damage resulted simply from probing by more aphids. Alternatively, higher RWASA2 population levels and feeding damage may be the consequence of longer bouts of feeding by this biotype. This study has provided no evidence in support of a difference in salivary biochemistry in the two biotypes, as has been proposed previously (Jimoh et al., 2011).

RWASA2 was initially discovered in the field because of its ability to feed and reproduce effectively on wheat containing the *Dn1* resistance gene (Tolmay et al., 2007). These authors suggested that RWASA2 virulence on *Dn1* wheat plants arose from a "gene for gene" interaction between a specific R-gene and a modified avirulence protein in the aphid's saliva (see Edwards and Singh, 2006). Widespread deployment of R-genes in crops can often select for virulent biotypes that are capable of successfully colonising resistant plants (Porter et al., 1997; Quick et al., 2001; Gatehouse, 2002). If this was the case, RWASA2 should not outperform RWASA1 on plants that do not contain the *Dn1* gene. Populations of RWASA2 grow faster than RWASA1 populations on susceptible wheat (Walton and Botha, 2008) and on susceptible and resistant barley (Jimoh et al., 2011). It is possible that the only biological difference between RWASA2 and RWASA1 is a higher reproductive rate.

The results of this study support our previous conclusions (Jimoh et al., 2011) that resistance to RWA in these STARS lines is not characteristic of R-gene resistance, and that the RWASA2 virulence phenotype on barley has not developed under a gene for gene model. We have also shown that there is a tolerance component to the resistance in these lines in addition to the antibiosis effect described previously (Jimoh et al., 2011). Based on this, these STARS lines represent an excellent potential source of durable resistance to RWA for the South African barley industry.

Acknowledgements

We thank Dr. V. Tolmay and Dr. G. Prinsloo from the ARC-Small Grain Institute, Bethlehem, South Africa for the supply of seeds and aphids and Dr. D. W. Mornhinweg of the USDA-ARS, Stillwater, Oklahoma, United States of America for

Fig. 7. RWASA2 feeding on resistant STARS lines. A. STARS-0502B. Thick-walled sieve tubes (solid circles) and adjacent vascular parenchyma in an intermediate vascular bundle were obliterated by saliva (SS) during this probe. Surrounding phloem tissue is partially plasmolysed. Xylem vessels and their pit membranes are occluded by saliva. B. STARS-0502B. Detail of probed xylem vessel from A. The thick, electron-dense saliva has encrusted walls (arrows) and pit membranes (double arrows). Punctured thick-walled sieve tube (centre left) is filled with saliva (SS) and surrounding vascular parenchyma cells are severely plasmolysed. C. STARS-9301B. Detail showing extensive, general plasmolysis of parenchyma and thin-walled sieve tubes (S). Metaxylem (MXV, right), cell walls and pit membranes are encrusted with electron dense saliva. D. STARS 9301B. Here, saliva lines the cell walls (SS). Metaxylem pit membranes (double arrows) are occluded. E. STARS-9577B. Vascular parenchyma cells (above) and thin-walled sieve tubes, companion and vascular parenchyma cells are extensively damaged. Complete disruption is evident in the cytoplasm of the companion cell (CC). Sieve tube cell walls are lined with saliva and callose is associated with the lateral sieve area pores (arrows). F. Detail from E. This pair of sieve tubes was disrupted by RWASA2 during feeding. Material associated with the lateral sieve area pores is presumably a mixture of callose and saliva. Abbreviations. BS = bundle sheath cell; CC = companion cell; MS = mestome sheath cell; MXV = large metaxylem vessel; S = thin-walled sieve tube; SM = salivary material; SS = stylet sheath; VP = vascular parenchyma cell; XV = xylem vessel; solid dot = thick-walled sieve tube.

permission to use seeds of the resistant STARS lines. We also thank S. Pinchuk and M. Randall of Electron Microscopy Unit, Rhodes University, Grahamstown for technical assistance with transmission electron microscopy. We gratefully acknowledge the assistance of Dr. S. Vetter and Prof. M. Villet respectively of the Departments of Botany and Zoology and Entomology, Rhodes University, Grahamstown, South Africa, for assistance with data analyses. The National Research Foundation (NRF), Pretoria and the Joint Research Committee, Rhodes University, Grahamstown, South Africa are acknowledged for continued support of CEJB's research programme and Mellon Scholarship award to MA Jimoh.

References

Botha, C.E.J., 2005. Interaction of phloem and xylem during phloem loading — functional symplasmic roles for thin- and thick-walled sieve tubes in monocotyledons? In: Holbrook, N.M., Zweiniecki, M.A. (Eds.), Vascular Transport in Plants. Elsevier, London, pp. 115–130.

Botha, C.E.J., Matsiliza, B., 2004. Reduction in transport in wheat (*Triticum aestivum*) is caused by sustained phloem feeding by the Russian wheat aphid (*Diuraphis noxia*). South African Journal of Botany 70, 249–254.

de Wet, L.R., Botha, C.E.J., 2007. Resistance or tolerance: an examination of aphid (*Sitobion yakini*) phloem feeding on Betta and Betta-Dn wheat (*Triticum aestivum*). South African Journal of Botany 73, 35–39.

Edwards, O., Singh, K.B., 2006. Resistance to insect pests: what do legumes have to offer? Euphytica 147, 273–285.

Evert, R.F., Eschrich, W., Eichhorn, S.E., Limbach, S.T., 1973. Observation on penetration of barley leaves by the aphid *Rhopalosiphum maidis* (Fitch). Protoplasma 77, 95–110.

Fouché, A., Verhoeven, R.L., Hewitt, P.H., Walters, M.C., Kriel, C.F., De Jager, J., 1984. Russian wheat aphid (*Diuraphis noxia*) feeding damage on wheat, related cereals and a bromus grass species. In: Walters, M.C. (Ed.), Progress in Russian Wheat Aphid (*Diuraphis noxia*, Mordvilko) Research in the Republic of South Africa. Technical Communication, vol. 191. Department of Agriculture, Republic of South Africa, pp. 22–33.

Gatehouse, J.A., 2002. Plant resistance towards insect behaviours: a dynamic interaction. New Phytologist 156, 145–169.

Hewitt, E.J., 1966. Sand and water culture methods used in the study of plant nutrition, 2nd Edition. Technical Communications, No. 22. Commonwealth Agricultural Bureau, Farnham, England.

Jimoh, M.A., Botha, C.E.J., Edwards, O., Bradley, G., 2011. Population growth rate and relative virulence of the two South African biotypes of Russian wheat aphid, *Diuraphis noxia*, and bird cherry-oat aphid, *Rhopalosiphum padi*, on resistant and non-resistant barley. Entomologia Experimentalis et Applicata 138, 12–20.

Johnson, R.A., Wichern, D.W., 2002. Applied Multivariate Statistical Analysis, 5th Edition. Prentice Hall, Upper Saddle River, New Jersey.

Jyoti, J.L., Qureshi, J.A., Michaud, J.P., Martin, T.J., 2006. Virulence of two Russian wheat aphid biotypes to eight wheat cultivars at two temperatures. Crop Science 46, 774–780.

Kovalev, O.V., Poprawski, T.J., Stekolshchikov, A.V., Vereshchgina, A.B., Grandbur, S.A., 1991. *Diuraphis aizenberg* (Homoptera: Aphididae): key to apterous viviparous females, and a review of Russian language literature on the natural history of *Diuraphis noxia* (Kurdjumov 1913). Journal of Applied Entomology 112, 425–436.

Kruger, G.H.J., Hewitt, P.H., 1984. The effect of Russian wheat aphid (*Diuraphis noxia*) extract on photosynthesis of isolated chloroplasts: preliminary studies. In: Walters, M.C. (Ed.), Progress in Russian Wheat Aphid (*Diuraphis noxia*, Mordvilko) Research in the Republic of South Africa. Technical Communication, No. 191. Department of Agriculture, Republic of South Africa, pp. 34–37.

Matsiliza, B., Botha, C.E.J., 2002. Aphid (*Sitobion yakini*) investigation suggests thin-walled sieve tubes in barley (*Hordeum vulgare*) to be more functional than thick-walled sieve tubes. Physiologia Plantarum 115, 137–143.

Mornhinweg, D.W., Porter, D.R., Webster, J.A., 1995. Registration of STARS-9301B Russian wheat aphid resistant barley germplasm. Crop Science 35, 602.

Mornhinweg, D.W., Porter, D.R., Webster, J.A., 1999. Registration of STARS-9577B Russian wheat aphid resistant barley germplasm. Crop Science 39, 882–883.

Mornhinweg, D.W., Obert, D.E., Wesenberg, C.A., Erickson, C.A., Porter, D.R., 2006. Registration of seven winter feed barley germplasms resistant to Russian wheat aphid. Crop Science 46, 1826–1827.

Porter, D.R., Burd, J.D., Shufran, K.A., Webster, J.A., Teetes, G.L., 1997. Greenburg (Homoptera: Aphididae) biotypes: selected by resistant cultivars or preadapted opportunists? Journal of Economic Entomology 90, 1055–1065.

Puterka, G.J., Burd, J.D., Mornhinweg, D.W., Haley, S.D., Peairs, F.B., 2006. Response of resistant and susceptible barley to infestations of five *Diuraphis noxia* (Homoptera: Aphididae) biotypes. Journal of Economic Entomology 99, 2151–2155.

Puterka, G.J., Burd, J.D., Porter, D., Shufran, K., Cheryl, B., Bowling, B., Patrick, C., 2007. Distribution and diversity of Russian wheat aphid (Hemiptera: Aphididae) biotypes in North America. Journal of Economic Entomology 100, 1679–1684.

Quick, J.S., Stromberger, J.A., Clayshulte, S., Johnson, J.J., Peairs, F.B., Rudolph, J.B., Lorenz, K., 2001. Registration of 'Prairie red' wheat. Crop Science 41, 1362–1363.

Saheed, S.A., Botha, C.E.J., Liu, L., Jonsson, L., 2007a. Comparison of structural damage caused by Russian wheat aphid (*Diuraphis noxia*) and Bird cherry-oat aphid (*Rhopalosiphum padi*) in a susceptible barley cultivar, *Hordeum vulgare* cv. clipper. Physiologia Plantarum 129, 429–435.

Saheed, S.A., Liu, L., Jonsson, L., Botha, C.E.J., 2007b. Xylem – as well as phloem – sustains severe damage due to feeding by the Russian wheat aphid. South African Journal of Botany 73, 593–599.

Saheed, S.A., Cierlik, I., Larsson, K.A.E., Delp, G., Bradley, G., Jonsson, L.M.V., Botha, C.E.J., 2009. Stronger induction of callose deposition in barley by Russian wheat aphid than Bird cherry-oat aphid is not associated with differences in callose synthase or β-1,3-glucanase transcript abundance. Physiologia Plantarum 135, 150–161.

Saheed, S.A., Jonsson, L.M.V., Botha, C.E.J., 2010. Russian wheat aphid causes greater reduction in phloem transport capacity of barley leaves than bird cherry-oat aphid. Acta Botanica Croatica 69, 7–18.

Spurr, A.R., 1969. A low-viscosity epoxy resin embedding medium for electron microscopy. Journal of Ultrastructure Research 26, 31–43.

Tjalingii, W.F., 1994. Sieve element acceptance by aphids. European Journal of Entomology 91, 47–52.

Tolmay, V.L., Lindeque, R.C., Prinsloo, G.J., 2007. Preliminary evidence of a resistance-breaking biotype of the Russian wheat aphid, *Diuraphis noxia* (Kurdjumov) (Homoptera: Aphididae), in South Africa. African Entomology 15, 228–230.

Walters, M.C., Penn, F., Du Toit, F., Botha, T.C., Aalbersberg, K., Hewitt, P.H., Broodryk, S.W., 1980. The Russian wheat aphid. Farming in South Africa, Leaflet Series, Wheat, G3, pp. 1–6.

Walton, S.M., Botha, C.E.J., 2008. The effects of two different biotypes (SA-1 and SA-2) of Russian wheat aphid, *Diuraphis noxia* (Kurdjumov) (Homoptera: Aphididae) on non-resistant and resistant wheat cultivars Tugela and Tugela-*Dn* (*Triticum aestivum*). Proceedings of the 23rd International Congress on Entomology (ICE), p. 2029.

Webster, J.A., Porter, D.R., Baker, C.A., Mornhinweg, D.W., 1993. Resistance to Russian wheat aphid (Homoptera: Aphididae) in barley: effects on aphid feeding. Journal of Economic Entomology 86, 1603–1608.

Edited by J Van Staden